

Dynamics of Random Graphs with Bounded Degrees

E. Ben-Naim¹ and P. L. Krapivsky²

¹*Theoretical Division and Center for Nonlinear Studies,*

Los Alamos National Laboratory, Los Alamos, New Mexico 87545, USA

²*Department of Physics, Boston University, Boston, Massachusetts 02215, USA*

We investigate the dynamic formation of regular random graphs. In our model, we pick a pair of nodes at random and connect them with a link if both of their degrees are smaller than d . Starting with a set of isolated nodes, we repeat this linking step until a regular random graph, where all nodes have degree d , forms. We view this process as a multivariate aggregation process, and formally solve the evolution equations using the Hamilton-Jacobi formalism. We calculate the nontrivial percolation thresholds for the emergence of the giant component when $d \geq 3$. Also, we estimate the number of steps until the giant component spans the entire system and the total number of steps until the regular random graph forms. These quantities are non self-averaging, namely, they fluctuate from realization to realization even in the thermodynamic limit.

PACS numbers: 02.50.-r, 05.40.-a, 89.75.Hc, 64.60.ah

I. INTRODUCTION

A random graph is a set of nodes that are connected by random links [1–4]. When the number of links exceeds a certain threshold, a giant component with a finite fraction of all nodes emerges [5, 6]. Therefore, random graphs are equivalent to a mean-field percolation process [7, 8]. Random graphs underlie many natural phenomena from polymerization [9–11] to the spread of infectious diseases [12–14], and they are also used to model social networks [15–17] as well as complexity of algorithms [18].

The classical random graph has no restrictions on the degree of a node. In many situations, the number of connections is limited, and specifically, the degree of each node must be bounded. Examples include the percolating network of contacts in a bead pack [19], computer networks [20], and communication networks [21].

We modify the canonical model for an evolving random graph [2–4, 22–24] by imposing a strict bound on the degree of a node [25, 26]. In an evolving random graph, two nodes are picked at random, and regardless of their degrees, the nodes are connected by a link. At the end of this process, a complete graph forms. In this study, we focus on a constrained process where the two nodes are linked only if both degrees are smaller than d . Starting with a set of N isolated nodes, the final state is a regular random graph [27, 28], where all nodes have degree d (Fig. 1). The evolving graph includes two types of nodes, active nodes with degree smaller than the maximum, and inactive nodes with the maximal degree. We obtain the density of active nodes from the full degree distribution, which is shown to be a truncated Poisson distribution.

In general, the graph is a set of disjoint connected components [29]. In each component, any two nodes are connected by a path. As in classical random graphs, our graphs could be in one of two phases — a non-percolating phase where all components are finite, and a percolating phase where a single *giant* component with a macroscopic number of nodes coexists with finite components. The transition between these two phases occurs when the

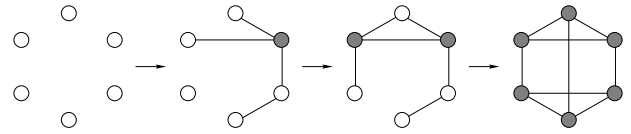


FIG. 1: Illustration of the linking process. Empty circles indicate active nodes, and filled circles depict inactive nodes. The initial state is a set of isolated nodes (left), while the final state is a regular random graph (right). As links are added, connected components form, and eventually, a single connected component spans the entire system.

number of links exceeds a threshold. For example, when $d = 3$, the critical link density, L_g , is

$$L_g = 0.577200. \quad (1)$$

When $d = 1$ the final state consists of dimers, while when $d = 2$ the final state includes multiple rings [30, 31]. In both cases, the system does not condense into a single component. We study the more interesting situation $d \geq 3$ where the system undergoes a percolation transition and the final state is a fully connected graph.

As a result of the linking process, connected components undergo an aggregation process. In the traditional binary aggregation framework [32, 33], connected components are characterized by the total number of nodes [22–24]. In our process, however, this minimal description does not lead to closed evolution equations. Instead, we describe clusters by the total number of nodes of degree $0, 1, \dots, d$. This complete description naturally lends itself to closed evolution equations. We use the elegant Hamilton-Jacobi method to obtain a formal solution for the density of connected components, and find the percolation thresholds from this solution.

We also use the degree distribution to illuminate the behavior during the late stages of the evolution. The regular random graph forms via a two-step process. First, the giant component takes over the entire system. This step occurs after T linking attempts, with

$T \sim N/(\ln N)^{d-1}$. At this point, only a small minority of the nodes in the giant component remain active. The total number of active nodes, M , scales logarithmically with system size,

$$M \sim (\ln N)^{d-1}. \quad (2)$$

Eventually all nodes become inactive, and the regular random graph is complete. The number of linking attempts required to reach this final state is proportional to the system size. Hence, the evolution of the regular random graph is much slower than the evolution of the classical random graph, where T is logarithmic in N [24].

The rest of this paper is organized as follows. The degree distribution is derived in section II. We then show that the linking process is equivalent to a multivariate aggregation process (Sec. III). A formal solution is obtained in Sec. IV using the Hamilton-Jacobi method. The emergence of the giant component is discussed in section V. In particular, the mass of the giant component is obtained as a function of time. The late-time kinetics including the emergence of a fully connected graph and a perfect regular random graph are described in section VI. We discuss the results in section VII. In Appendix A, we rederive relevant properties of classical random graphs using the Hamilton-Jacobi method.

II. DEGREE DISTRIBUTION

We study a random process that generates a regular random graph. The process starts at time $t = 0$ with N disconnected nodes. At each elementary step, two nodes are chosen at random. If the degrees of the two nodes are both smaller than d , a new link connects them; otherwise, no link is added. Time is augmented by $2/N$ after each linking attempt, $t \rightarrow t + 2/N$, so that every node participates in one linking attempt per unit time, on average. Linking is repeatedly attempted until a regular random graph forms (Fig. 1).

There are two types of nodes — active nodes with degree smaller than d and inactive nodes with degree equal to d . A new link between two active nodes of degrees $i < d$ and $j < d$ augments the degrees:

$$(i, j) \rightarrow (i + 1, j + 1). \quad (3)$$

This random process occurs with unit rate. The linking process (3) transforms the system from a set of active nodes into a set of inactive nodes, as illustrated on Fig. 1.

Let $n_j(t)$ be the degree distribution, that is, the fraction of nodes with degree j at time t . The degree distribution is properly normalized, $\sum_{j=0}^d n_j = 1$, and its partial sum gives the total density of active nodes, ν ,

$$\nu = \sum_{j=0}^{d-1} n_j. \quad (4)$$

The density of active nodes controls the process: the degree distribution obeys the rate equations

$$\frac{dn_j}{dt} = \begin{cases} \nu(n_{j-1} - n_j) & j < d, \\ \nu n_{d-1} & j = d. \end{cases} \quad (5)$$

The initial condition is

$$n_j(0) = \delta_{j,0}, \quad (6)$$

and the “boundary” condition $n_{-1} \equiv 0$ ensures that $dn_0/dt = -\nu n_0$. Equations (5) are nonlinear because (3) is a two-body process. Yet, since the density ν merely sets the overall linking rate, we can linearize Eqs. (5) by introducing the time variable

$$\tau = \int_0^t dt' \nu(t'), \quad (7)$$

or equivalently, $d\tau/dt = \nu$. In terms of the time variable τ , the rate equations become

$$\frac{dn_j}{d\tau} = \begin{cases} n_{j-1} - n_j & j < d, \\ n_{d-1} & j = d. \end{cases} \quad (8)$$

We use the initial condition (6) and solve (8) recursively to find $n_0 = e^{-\tau}$, $n_1 = \tau e^{-\tau}$, $n_2 = \frac{1}{2}\tau^2 e^{-\tau}$, etc. Therefore, the degree distribution is a truncated Poisson distribution [34]

$$n_j = \frac{\tau^j}{j!} e^{-\tau}, \quad (9)$$

for $j < d$. The density of inactive nodes, $n_d = 1 - \nu$, follows from the normalization condition. From the definitions (4) and (7), the time variable τ obeys the nonlinear ordinary differential equation

$$\frac{d\tau}{dt} = \sum_{j=0}^{d-1} \frac{\tau^j}{j!} e^{-\tau}, \quad (10)$$

with the initial condition $\tau(0) = 0$. Equations (9) and (10) specify the degree distribution.

The time evolution of the degree distribution, obtained by numerical integration of (10) for the case $d = 3$, is shown in Fig. 2. As expected, the density of isolated nodes, $n_0(t)$, declines monotonically, while the density of inactive nodes, $n_3(t)$, increases monotonically. Isolated nodes initially dominate, then nodes with degree one are most numerous, and eventually, inactive nodes take the lead for good.

The average degree, $\langle j \rangle = \sum_{j=0}^d j n_j$, characterizes the overall connectivity. Since every link connects two nodes, the density of links, L , is proportional to the average degree, $L = \langle j \rangle / 2$. By multiplying (8) by j and summing over j , we see that the average degree satisfies

$$\frac{d\langle j \rangle}{d\tau} = \nu. \quad (11)$$

Using the initial and final values, $\langle j \rangle_0 = 0$ and $\langle j \rangle_\infty = d$, we have the integral identity $\int_0^\infty d\tau \nu(\tau) = d$.

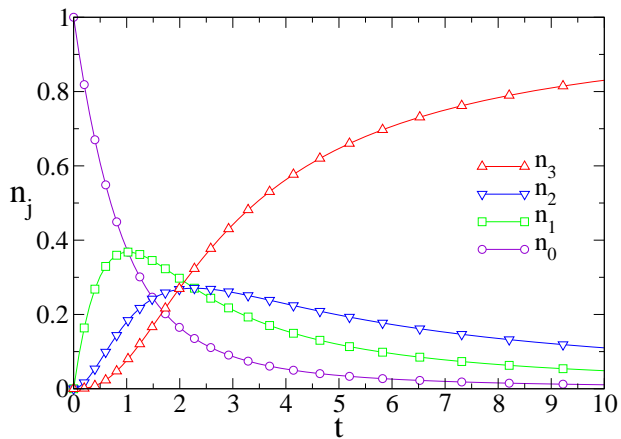


FIG. 2: The degree distribution $n_j(t)$ versus time t for $d = 3$.

III. MULTIVARIATE AGGREGATION

Every node belongs to a connected component, or “cluster”. Initially, there are N clusters, and eventually, a single cluster remains. The number of clusters dwindles as a result of a cluster-cluster aggregation [35] process: any link between two active nodes in separate clusters merges the two clusters. Since the aggregation rate depends on the total number of *active* nodes, characterization of clusters by their total size is insufficient. Adding the number of active nodes as a second variable does not lead to a closed description either, because the number of active nodes may change once a link is added. Therefore, we use a complete description and characterize clusters by $(d + 1)$ -dimensional vectors

$$\mathbf{k} \equiv (k_0, k_1, \dots, k_d), \quad (12)$$

where k_j is the number of nodes of degree j . The cluster size, k , is simply $k \equiv |\mathbf{k}| = k_0 + k_1 + \dots + k_d$. Finite clusters are typically trees [36]. Since there are $k - 1$ links in a tree of size k , we have the constraint

$$2(k - 1) = k_1 + 2k_2 + \dots + dk_d.$$

In particular, minimal clusters with $\mathbf{k} = (1, 0, \dots, 0)$ trivially satisfy this condition.

As a result of the linking process (3), clusters undergo the multivariate aggregation process

$$\mathbf{l}, \mathbf{m} \xrightarrow{l_i m_j} \mathbf{l} + \mathbf{m} + \mathbf{e}_i + \mathbf{e}_j, \quad (13)$$

with $i < d$ and $j < d$. Here, the vector \mathbf{e}_j describes the degree augmentation $j \rightarrow j + 1$,

$$\begin{aligned} \mathbf{e}_0 &= (-1, 1, 0, 0, \dots, 0), \\ \mathbf{e}_1 &= (0, -1, 1, 0, \dots, 0), \\ &\vdots \\ \mathbf{e}_{d-1} &= (0, 0, \dots, 0, -1, 1). \end{aligned}$$

The aggregation rate $l_i \times m_j$ in (13) equals the product of the number of nodes of degree i in the first cluster and the number of nodes of degree j in the second cluster.

The density $c(\mathbf{k}, t)$ of clusters with “size” \mathbf{k} at time t obeys the rate equation

$$\frac{dc(\mathbf{k})}{dt} = \frac{1}{2} \sum_{\substack{\mathbf{l}, \mathbf{m} \\ i, j < d}} l_i m_j c(\mathbf{l}) c(\mathbf{m}) \delta_{\mathbf{k}, \mathbf{l} + \mathbf{m} + \mathbf{e}_i + \mathbf{e}_j} - \nu \left(\sum_{j=0}^{d-1} k_j \right) c(\mathbf{k}),$$

where ν is the density of active nodes (4). Henceforth, the time dependence is implicit. The gain term directly reflects the aggregation process (13), and the factor $1/2$ prevents over-counting. The loss rate is proportional to the total number of active nodes in the cluster, as well as the density of active nodes in the entire system.

A crucial feature of the above rate equation is that the gain term and the loss term are different in nature. The gain term, which describes creation of clusters with finite size, is proportional to the product of cluster densities. The loss term, which describes loss of finite clusters due to linking, is proportional to the product of the cluster density and the total density of active nodes in the entire system, which does take into account the giant component, if one exists. For this reason, the rate equation is valid in the non-percolating phase as well as in the percolating phase.

In terms of the time variable τ , the loss term becomes linear

$$\frac{dc(\mathbf{k})}{d\tau} = \frac{1}{2\nu} \sum_{\substack{\mathbf{l}, \mathbf{m} \\ i, j < d}} l_i m_j c(\mathbf{l}) c(\mathbf{m}) \delta_{\mathbf{k}, \mathbf{l} + \mathbf{m} + \mathbf{e}_i + \mathbf{e}_j} - \left(\sum_{j=0}^{d-1} k_j \right) c(\mathbf{k}). \quad (14)$$

The initial condition is $c(\mathbf{k}, 0) = \delta_{\mathbf{k}, (1, 0, \dots, 0)}$. The rate equations for the cluster size distribution are nonlinear, in contrast with the linear equations (8) for the degree distribution. Moreover, the rate equations (14) are substantially more challenging than those previously analyzed in studies of multivariate aggregation processes [37, 38].

The generating function approach is generally useful in aggregation problems [24, 35, 39, 40], and in our case, we must use the multivariate generating function

$$C(\mathbf{x}, \tau) = \sum_{\mathbf{k}} c(\mathbf{k}, \tau) \mathbf{x}^{\mathbf{k}}. \quad (15)$$

Here $\mathbf{x} \equiv (x_0, x_1, \dots, x_d)$ and $\mathbf{x}^{\mathbf{k}} \equiv x_0^{k_0} x_1^{k_1} \dots x_d^{k_d}$ is a shorthand for the product of monomials. Multiplying (14) by $\mathbf{x}^{\mathbf{k}}$ and performing the summation over \mathbf{k} , we find that the generating function evolves according to

$$\frac{\partial C}{\partial \tau} = \frac{1}{2\nu} \left(\sum_{j=0}^{d-1} x_{j+1} \frac{\partial C}{\partial x_j} \right)^2 - \sum_{j=0}^{d-1} x_j \frac{\partial C}{\partial x_j}. \quad (16)$$

The initial condition is

$$C(\mathbf{x}, 0) = x_0. \quad (17)$$

IV. HAMILTON-JACOBI FORMULATION

The generating function satisfies a non-linear Partial Differential Equation (PDE) with non-constant coefficients. Crucially, equation (16) is a *first-order* PDE, and hence, it can be reduced to a set of coupled Ordinary Differential Equations (ODEs) by applying the method of characteristics [41, 42]. This is a significant simplification as a PDE is essentially a collection of infinitely many ODEs. Moreover, in the present case, we conveniently treat the governing equation as a *Hamilton-Jacobi* equation, thereby bypassing the method of characteristics [41, 43]. Then, the canonical Hamilton equations coincide with the equations for the characteristics.

First, we convert (16) into a Hamilton-Jacobi equation

$$\frac{\partial C(\mathbf{x}, \tau)}{\partial \tau} + H(\mathbf{x}, \nabla C, \tau) = 0 \quad (18)$$

and view $C(\mathbf{x}, \tau)$ and $H(\mathbf{x}, \nabla C, \tau)$ as “action” and “Hamiltonian”, respectively. Second, we treat \mathbf{x} as “coordinate”, and ∇C as “momentum”, $\mathbf{p} = \nabla C$; in components, $p_j = \frac{\partial C}{\partial x_j}$ for all j . The Hamiltonian is

$$H(\mathbf{x}, \mathbf{p}, \tau) = \sum_{j=0}^{d-1} x_j p_j - \frac{\Pi_1^2}{2\nu(\tau)}, \quad (19)$$

where for convenience, we introduced a set of auxiliary functions,

$$\Pi_j = \sum_{i=j}^d x_i p_{i-j}, \quad (20)$$

for all j . We stress that the Hamiltonian (19) is not a conserved quantity because of the explicit dependence on time τ , which enters via $\nu(\tau)$. The Hamilton-Jacobi equation (18) is equivalent to the canonical Hamilton equations

$$\frac{dx_j}{d\tau} = \frac{\partial H}{\partial p_j}, \quad \frac{dp_j}{d\tau} = -\frac{\partial H}{\partial x_j}. \quad (21)$$

Hence, the non-linear partial differential equation (16) reduces to $2(d+1)$ coupled ordinary differential equations for the coordinates x_j and the momenta p_j .

From (21) and (19), the evolution equations for the momenta are

$$\frac{dp_j}{d\tau} = \begin{cases} \frac{\Pi_1}{\nu} p_{j-1} - p_j & j < d, \\ \frac{\Pi_1}{\nu} p_{d-1} & j = d. \end{cases} \quad (22)$$

The initial condition $p_j(0) = \delta_{j,0}$ follows from $\mathbf{p} = \nabla C$ and (17), and the boundary condition is $p_{-1} \equiv 0$. The structure of the *linear* equations (22) for p_j is identical to that of equations (8) for n_j , and the initial conditions are the same, too. By integrating equations (22) recursively, we find

$$p_j = \frac{u^j}{j!} e^{-\tau} \quad (23)$$

for $j < d$, with function u defined by

$$u = \int_0^\tau d\tau' \frac{\Pi_1(\tau')}{\nu(\tau')}, \quad (24)$$

or alternatively, $du/d\tau = \Pi_1/\nu$. To determine p_d , we rewrite the last equation in (22) as $dp_d/du = p_{d-1}$, and therefore, $p_d = \int_0^u du' p_{d-1}(u')$. Formally, the momenta p_j resemble the degree distribution n_j .

Using (21) and (19), the evolution equations for the coordinates are

$$\frac{dx_j}{d\tau} = \begin{cases} x_j - \frac{\Pi_1}{\nu} x_{j+1} & j < d, \\ 0 & j = d. \end{cases} \quad (25)$$

The initial condition is $\mathbf{x}(\tau = 0) = \mathbf{y}$. One of the coordinates does not change, $x_d = y_d$. We may integrate (25) and solve for the final coordinate \mathbf{x} as a function of the initial coordinate \mathbf{y} . Yet, as shown below, we need to solve the inverse problem — find \mathbf{y} as a function of \mathbf{x} .

Fortunately, the auxiliary functions defined in (20) enable us to accomplish this task. We first note that at time $\tau = 0$, these sums coincide with the initial coordinates, $\Pi_j(\tau = 0) = y_j$. Using the evolution equations (22) and (25), we calculate the evolution equations for Π_j ,

$$\begin{aligned} \dot{\Pi}_j &= \sum_{i=j}^d (\dot{x}_i p_{i-j} + x_i \dot{p}_{i-j}) \\ &= \sum_{i=j}^{d-1} (x_i - \frac{\Pi_1}{\nu} x_{i+1}) p_{i-j} + \sum_{i=j}^d x_i (\frac{\Pi_1}{\nu} p_{i-j-1} - p_{i-j}) \\ &= -x_d p_{d-j}, \end{aligned}$$

when $j > 0$. Here, the overdot is shorthand for time derivative, $\dot{\cdot} \equiv \frac{d}{d\tau}$. A similar calculation shows that Π_0 is conserved, $\dot{\Pi}_0 = 0$. Hence, the functions Π_j obey

$$\frac{d\Pi_j}{d\tau} = \begin{cases} 0 & j = 0, \\ -x_d p_{d-j} & j > 0. \end{cases} \quad (26)$$

The initial condition is $\Pi_j(0) = y_j$. Since the coordinate x_d is a constant, integration of these evolution equations is immediate, and using the initial condition $\Pi_j(0) = y_j$, we find [44]

$$y_j = \begin{cases} \sum_{i=0}^d x_i p_i & j = 0, \\ \sum_{i=j}^d x_i p_{i-j} + x_d \int_0^\tau d\tau' p_{d-j}(\tau') & j > 0. \end{cases} \quad (27)$$

(The lower expression holds up to $j = d$; indeed, using $p_0 = e^{-\tau}$ we recover $y_d = x_d$.) Equations (27), together with the known momenta (23), specify the initial coordinates in terms of the final coordinates. Remarkably, we formally solved the inverse problem!

To complete the solution of the Hamilton-Jacobi equations, we must specify the function u in (23). Using the definition (24), we calculate the second derivative of u ,

$$\frac{d^2 u}{d\tau^2} = \frac{d}{d\tau} \frac{\Pi_1}{\nu} = -x_d \frac{p_{d-1}}{\nu} + \frac{n_{d-1}}{\nu} \frac{du}{d\tau}.$$

Here, we used $d\nu/d\tau = -n_{d-1}$, as follows from (8). By multiplying the above equation by ν , and by substituting (9) and (23), we find that u satisfies a *closed* second-order ordinary differential equation,

$$\left(\sum_{j=0}^{d-1} \frac{\tau^j}{j!} \right) \frac{d^2 u}{d\tau^2} - \frac{\tau^{d-1}}{(d-1)!} \frac{du}{d\tau} + x_d \frac{u^{d-1}}{(d-1)!} = 0. \quad (28)$$

The initial conditions are $u(0) = 0$ and $du(0)/d\tau = y_1$. This equation is linear if and only if $d \leq 2$.

However, we still do not know y_1 because the initial coordinates are coupled to the function u , according to (27). To find y_1 , we have to integrate equation (28), starting with trial initial conditions $u(0) = 0$ and $du(0)/d\tau = y_1^*$, and find the root of the integral equation

$$y_1^* = \sum_{i=1}^d x_i p_{i-1} + x_d \int_0^\tau d\tau' p_{d-1}(\tau'). \quad (29)$$

The second order ODE (28) and the integral equation (29) specify the variable u and hence, the momenta p_j and the initial coordinates y_j via the explicit solutions (23) and (27). We stress that the function $u \equiv u(\mathbf{x}, \tau)$ depends on the coordinate \mathbf{x} .

Finally, we obtain the generating function (15) by evaluating its complete derivative with respect to τ ,

$$\begin{aligned} \frac{dC(\mathbf{x}, \tau)}{d\tau} &= \frac{\partial C}{\partial \tau} + \frac{\partial C}{\partial \mathbf{x}} \cdot \frac{d\mathbf{x}}{d\tau} = -H + \mathbf{p} \cdot \frac{\partial H}{\partial \mathbf{p}} \\ &= -\frac{\Pi_1^2}{2\nu} = -\frac{\nu}{2} \left(\frac{du}{d\tau} \right)^2. \end{aligned} \quad (30)$$

By integrating (30) subject to the initial condition $C(\mathbf{x}, 0) = y_0$, and recalling the conservation law $y_0 = \Pi_0$, we get

$$C(\mathbf{x}, \tau) = \sum_{j=0}^d x_j p_j - \frac{1}{2} \int_0^\tau d\tau' \nu(\tau') \left(\frac{du}{d\tau} \right)^2. \quad (31)$$

This expression, supplemented by equations (28) and (29) for u , as well as the explicit expressions (23) for the momenta, constitutes a formal solution for the generating function. Therefore, representation of the linking process as a multivariate aggregation process enables analytical treatment of the cluster-size distribution.

V. GIANT COMPONENT

By definition, the size distribution $c(\mathbf{k})$ describes finite connected components. However, the system may be in one of two phases — a *non-percolating* phase in which finite components contain all the mass, and a *percolating* phase in which a giant component, containing a fraction g of the entire mass, coexists with finite components. We expect that the giant component emerges suddenly, at a finite time t_g (see Appendix A).

The mass of the giant component g follows directly from the momenta when $\mathbf{x} = (1, 1, \dots, 1)$. Indeed, using (15), we have

$$1 - g = \sum_{\mathbf{k}} k c(\mathbf{k}) = \sum_{j=0}^d p_j, \quad (32)$$

or alternatively, $g = 1 - y_0$, as follows from the conservation law $\Pi_0 = y_0$. Hence, we substitute $x_d = 1$ into equation (28), and obtain the evolution equation for u ,

$$\left(\sum_{j=0}^{d-1} \frac{\tau^j}{j!} \right) \frac{d^2 u}{d\tau^2} - \frac{\tau^{d-1}}{(d-1)!} \frac{du}{d\tau} + \frac{u^{d-1}}{(d-1)!} = 0. \quad (33)$$

The initial conditions are $u(0) = 1$ and $du(0)/d\tau = y_1$. Also, when $\mathbf{x} = (1, 1, \dots, 1)$, the integral equation (29) becomes

$$y_1^* = \sum_{j=0}^{d-1} p_j + \int_0^\tau d\tau' p_{d-1}(\tau'), \quad (34)$$

with p_j given by (23).

First, there is the trivial solution $u = \tau$ and $y_j = 1$ for all j , for which the momenta equals the degree distribution, $p_j = n_j$. For this solution, $g = 0$, and the system is in the finite component phase. When $d \leq 2$, the trivial solution holds at all times. In the case $d = 1$ the final state is merely a collection of $N/2$ dimers; in the case $d = 2$, the final state includes only rings [30, 31]. In both of these cases the system does not condense into a single component.

When $d \geq 3$, there is a second nontrivial solution when $\tau > \tau_g$ or equivalently, $t > t_g$. To find the nontrivial solution, we solved equation (33) numerically, using Adams' method [45, 46], starting with a trial initial condition $u(0) = 0$ and $du(0)/d\tau = y_1^*$, and then found the root of the integral equation (34) using the bisection method [47]. (Conveniently, the integral equations may be converted into first-order differential equations [44].) We then obtained the mass of the giant component using (32). To evaluate time, t , and the average degree, $\langle j \rangle$, in terms of the modified time variable τ , we simply integrated $dt/d\tau = 1/\nu$ and equation (11).

For the case $d = 3$, we find the critical time $\tau_g = 1.197395$ that corresponds to

$$t_g = 1.243785. \quad (35)$$

When the giant component emerges, the average degree of a node is $\langle j \rangle_g = 1.154399$. Moreover, the critical density of links quoted in (1) is obtained from $L_g = \langle j \rangle_g / 2$. Thus, the fraction f_g of successful linking attempts is

$$f_g = \frac{\langle j \rangle_g}{t_g} = 0.928135. \quad (36)$$

Generally, the percolation parameters characterizing the phase transition from the finite component phase to the giant component phase are nontrivial.

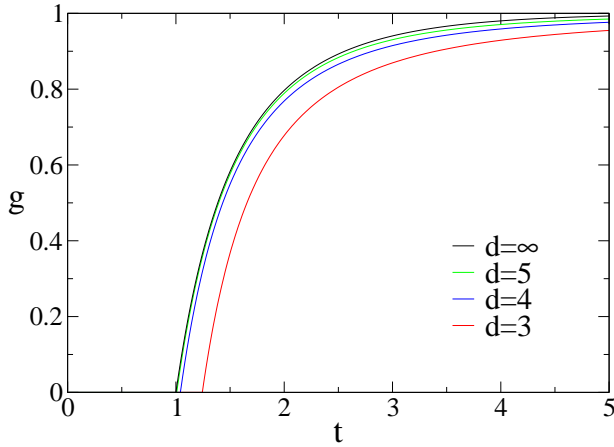


FIG. 3: The giant component mass $g(t)$ versus time t . Results of the Hamilton-Jacobi theory are shown for $d = 3, 4, 5$. Also shown as reference, is the solution to Eq. (A7) for the classical random graph, $d = \infty$

d	t_g	τ_g	$\langle j \rangle_g$	f_g	ν_g
3	1.243785	1.197395	1.154399	0.928135	0.880052
4	1.041130	1.035995	1.030922	0.990195	0.978725
5	1.007307	1.006593	1.005879	0.998582	0.996238
6	1.001169	1.001074	1.000978	0.999809	0.999403
7	1.000164	1.000152	1.000141	0.999977	0.999917
∞	1	1	1	1	1

TABLE I: Percolation parameters for $3 \leq d \leq 7$ and $d = \infty$. Listed are the time, t_g , the modified time, τ_g , the average degree, $\langle j \rangle_g = 2L_g$, the fraction of successful linking attempts, f_g , and the density of active nodes, ν_g , when the giant component emerges.

Table I lists the percolation parameters for $3 \leq d \leq 7$. Remarkably, the restriction on the degree of a node has a small effect on the percolation parameters already when $d = 4$. Moreover, as the maximal degree d increases, the percolation parameters quickly converge to the classical random graph values.

Figure 3 shows the mass of the giant component for $3 \leq d \leq 5$ and $d = \infty$. At moderate times, the quantity g converges to the classical random graph behavior (A7). Yet, as will be shown in the next section, the long-time evolution of the regular random graph is much slower compared with the classical random graph.

The function u at $\mathbf{x} = (1, 1, \dots, 1)$ also gives the total density of clusters, c , since $c = C(1, 1, \dots, 1)$. The formal solution (31) together with (32) give

$$c(\tau) = 1 - g(\tau) - \frac{1}{2} \int_0^\tau d\tau' \nu(\tau') \left(\frac{du}{d\tau} \right)^2. \quad (37)$$

Figure 4 shows that the concentration is a smooth function of time, even at the percolation point [48]. We also mention a useful relation between the cluster density and the link density throughout the non-percolating

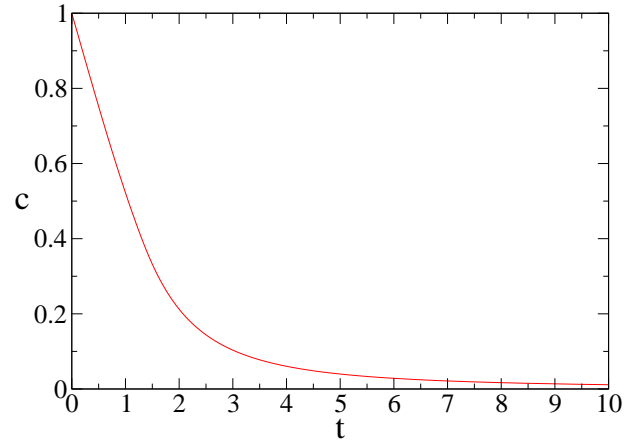


FIG. 4: The concentration $c(t)$ versus time t for the case $d = 3$.

phase. Every link reduces the number of clusters by one. Hence, $dc/dt = -dL/dt$, and consequently, $c + L = 1$ when $t \leq t_g$. In particular, $c_g + L_g = 1$.

Let c_k be the density of clusters with total size k , and let $\mathcal{C}(x) = \sum_k c_k x^k$ be the corresponding generating function. This single-variable generating function coincides with the multivariate counterpart (15) when all the coordinates are identical

$$\mathcal{C}(x) \equiv C(x, x, \dots, x). \quad (38)$$

Therefore, we have to vary x and obtain $u \equiv u(x)$ by solving the differential equation (28) along with the integral equation (29) with $x_i = x$ for all i . Finally, we substitute u into (31). We present results for the critical behavior, $\mathcal{C}_g(x) \equiv \mathcal{C}(x, \tau_g)$, and focus on the large- k behavior, that follows from (figure 5)

$$\mathcal{C}_g(x) = c_g - (1 - x) + B(1 - x)^{3/2} + \dots, \quad (39)$$

as $x \rightarrow 1$. The constant term is simply the critical concentration, $c_g = 1 - L_g = 1 - \langle j \rangle_g / 2$ (Table I). The linear term reflects the fact that finite clusters contain all the mass, $\mathcal{C}'(1) = \sum_k k c_k = 1$. Finally, the leading singular term $(1 - x)^{3/2}$ shows that $c_k \sim k^{-5/2}$ as follows from the Taylor series,

$$(1 - x)^{3/2} = \frac{3}{4\sqrt{\pi}} \sum_{k=0}^{\infty} \frac{\Gamma(k - 3/2)}{\Gamma(k + 1)} x^k,$$

and the limiting behavior $\Gamma(k + a) / \Gamma(k + b) \simeq k^{a-b}$ when $k \rightarrow \infty$. Hence, the critical cluster-size distribution has the power-law tail

$$c_k \simeq A k^{-5/2}, \quad (40)$$

with $A = 3B/4\sqrt{\pi}$ (see also Appendix A). Table II lists the prefactors B for $3 \leq d \leq 7$ and $d = \infty$. As a critical phenomenon [49], the evolving regular random graph is in the universality class of mean-field percolation [7].

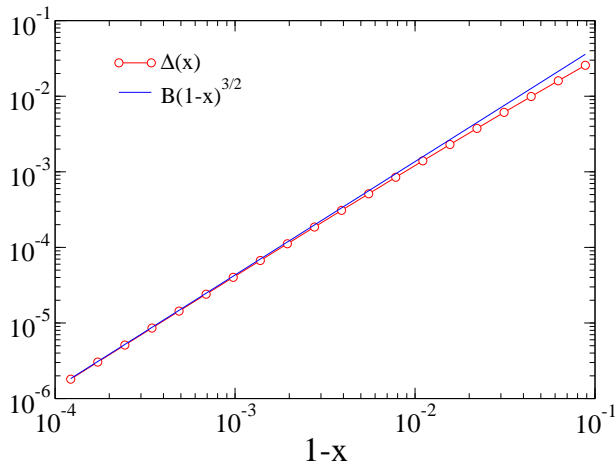


FIG. 5: The leading singular component of the generating function $\mathcal{C}_g(x)$ at the critical point. The quantity $\Delta(x) = \mathcal{C}_g(x) - c_g + (1-x)$ and the fit $B(1-x)^{3/2}$ are plotted versus $1-x$.

d	3	4	5	6	7	∞
B	1.368	1.037	0.962	0.944	0.943	0.942809

TABLE II: The prefactor B in (39) for $3 \leq d \leq 7$ and $d = \infty$. The last entry, $B = 2\sqrt{2}/3$, is from Eq. (A8).

VI. LARGE TIME BEHAVIOR

We now turn to the large-time behavior. This behavior largely follows from the degree distribution (9). We start with the crude estimate, $\tau \simeq \ln t$, obtained by replacing the right-hand-side of (10) with the dominant exponential term, $d\tau/dt = e^{-\tau}$. Then, we establish the corrections to this logarithmic behavior by keeping the leading term in (10)

$$\frac{d\tau}{dt} \simeq \frac{\tau^{d-1}}{(d-1)!} e^{-\tau}.$$

From this equation, we find the relation

$$\frac{\tau^{d-1}}{(d-1)!} e^{-\tau} \simeq t^{-1},$$

when $t \rightarrow \infty$. Substituting this expression into (9) gives the leading asymptotic behavior of the degree distribution

$$n_j \simeq \frac{(d-1)!}{j!} t^{-1} (\ln t)^{-(d-1-j)}, \quad (41)$$

for $j < d$. The densities of active nodes with degree $j < d-1$ decay algebraically with time, albeit with a logarithmic correction. Furthermore, the degree distribution is an increasing function of j . Since $\nu \simeq n_{d-1}$, the quantity ν exhibits the universal power-law decay

$$\nu \simeq t^{-1}. \quad (42)$$

The smaller the degree j , the faster the decay of n_j . In particular, the density of isolated nodes exhibits the fastest decay,

$$n_0 \simeq (d-1)! t^{-1} (\ln t)^{-(d-1)}. \quad (43)$$

Each isolated node represents a minimal cluster with size $k = 1$. Therefore (43) gives the density of minimal clusters. The asymptotic behavior (43) is much slower than the fast exponential decay found in ordinary random graphs [24]. Hence, the restriction on the degree leads to much slower long-time kinetics.

The asymptotic results (42) and (43) provide useful information about the final stages of the evolution. Amongst all clusters, minimal clusters survive the longest. Hence, when all minimal clusters disappear, a single cluster remains, and the giant component takes over the entire system. The time to reach a single component, T , grows with N according to

$$T \sim \frac{N}{(\ln N)^{d-1}}, \quad (44)$$

as follows from the “depletion” criterion $Nn_0 \sim 1$. This time is not self-averaging: it fluctuates from realization to realization. In particular, the average $\langle T \rangle$ does not give the second moment $\langle T^2 \rangle$; namely,

$$\lim_{N \rightarrow \infty} \frac{\langle T^2 \rangle}{\langle T \rangle^2} > 1. \quad (45)$$

This breakdown of self averaging is in sharp contrast with the behavior of ordinary random graphs where T is a self-averaging quantity. The conclusion (45) is based on the observation that a slight variation in the depletion criterion, say $Nn_0 \sim 2$, gives a different estimate for T .

When the giant component contains all N nodes, the vast majority of the nodes are inactive. Yet, a small majority of nodes remain active. Let M_j be the average number of nodes with degree $j > 0$ when the graph becomes fully connected for the first time [50]. This quantity grows logarithmically with system size (figure 6)

$$M_j \sim (\ln N)^j, \quad (46)$$

with $0 < j < d$, as follows from $M_j \simeq Nn_j(T)$, along with equations (41) and (44). The majority of active nodes have the largest possible degree, $j = d-1$. As stated in Eq. (2), the total number of active nodes, when the giant component first takes over the entire system, M , is logarithmic.

To test these predictions, we performed Monte-Carlo simulations. In the simulations, we start with N isolated nodes. At each step, we pick two *active* nodes and connect them. Keeping track of the active nodes maximizes computational efficiency, and allows us to simulate large systems with $N = 10^7$. We performed simulations for the case $d = 3$, and measured the average number of nodes with degree 1 and degree 2 when the graph condenses into a single component for the first time (figure 6). Also, we

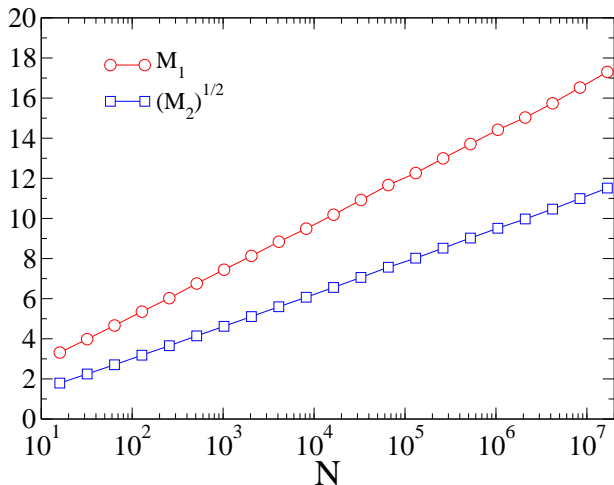


FIG. 6: The average number of active nodes when the graph becomes fully connected for the first time. Shown are M_1 and $M_2^{1/2}$ as a function of system size N , for the case $d = 3$. The results are from an average over 10^4 independent simulation runs.

verified that the time T fluctuates from realization to realization by measuring the ratio in (45).

The asymptotic behavior (41) indicates that there are several intermediate steps until the regular random graph fully forms. Isolated nodes disappear first, and at this time, there are $(\ln N)^{d-1}$ active nodes. Nodes with degree 1 disappear next, and at this point, $(\ln N)^{d-2}$ active nodes remain. There are d such steps, and in the last step, nodes with degree $d - 1$ disappear. Now, the regular random graph is complete. The time it takes to form the regular random graph is linear in system size,

$$t_f \sim N, \quad (47)$$

as follows from the depletion criterion $N\nu \sim 1$, and the algebraic decay (42). Like the quantity T , the formation time t_f is a fluctuating quantity, even in the limit $N \rightarrow \infty$.

For completeness, we also mention the asymptotic behavior of the cluster-size distribution,

$$c_k \sim t^{-1}(\ln t)^{-k(d-1)}, \quad (48)$$

in the long-time limit ($d = 2$ is a special case of a model considered in [51]). For minimal clusters, $c_1 = n_0$, and this behavior follows from the density of isolated nodes. The behavior (48) follows from the master equation

$$\frac{dc_k}{dt} = \frac{1}{2} \sum_{l+m=k} l m c_l c_m - \nu k c_k, \quad (49)$$

for $k \leq d$. Except for the loss rate, which is proportional to the overall density of active nodes, ν , this rate equation is the same as (A1). Clusters with $k \leq d$ contain only active nodes, and hence, the loss term is proportional to cluster size, k . Starting with $c_1 \sim t^{-1}(\ln t)^{-(d-1)}$,

the leading asymptotic behavior (48) can be established recursively from equation (49).

In general, we must classify clusters by their topology, and construct specific rate equations for each topology. The resulting rate equations have the same overall structure as (49) and as a consequence, the asymptotic behavior (48) appears to hold also when $k > d$. The proportionality constants depend on cluster topology, however. Finally, we note that the criterion $Nc_k \sim 1$ shows that the asymptotic behavior (48) is relevant only in a limited range of sizes, $k \ll k_*$ with the logarithmic cutoff $k_* \simeq (d - 1)^{-1} \ln N$. The cluster size distribution is sharply suppressed beyond the cutoff k_* .

VII. DISCUSSION

In conclusion, we studied the evolution of random graphs with a bounded degree using a dynamic linking process. First, a giant component, which contains a macroscopic number of nodes, emerges in a finite time. We obtained the nontrivial thresholds for this percolation transition. Then, the giant component takes over the entire system. The evolution still proceeds as some nodes have yet to reach the maximal degree. While the number of linking attempts before the giant component emerges is a self-averaging quantity, the number of steps it takes to form a fully connected graph or to complete the regular random graph are both fluctuating (non-self-averaging) quantities.

The regular random graph is completed via multiple steps. In the first step, nodes with degree 0 disappear and at the point, the graph is fully connected. Then, nodes with degree 1 disappear, etc. The total number of nodes with degree $d - 1$ diminishes by a factor $\ln N$ in each step,

$$(\ln N)^{d-1} \rightarrow (\ln N)^{d-2} \rightarrow \dots \rightarrow (\ln N) \rightarrow 0.$$

Similarly, the number of nodes of degree $d - 2$ shrinks according to $(\ln N)^{d-2} \rightarrow (\ln N)^{d-3} \rightarrow \dots$. Furthermore, the asymptotic behavior (49) indicates a multitude of time scales. Clusters of size k disappear at time

$$T_k \sim \frac{N}{(\ln N)^{k(d-1)}},$$

for all $k \ll k_*$. The time $T \equiv T_1$ is simply the largest in a series of time scales, $T_1 > T_2 > T_3 > \dots$. Therefore, multiple finite-size scaling laws characterize kinetics of regular random graphs.

The evolution equation for the cluster-size density is not a closed equation. To address this challenge, we introduced the multivariate size distribution, where the number of nodes with a given degree is specified. For this quantity, the evolution equations are closed. Using the Hamilton-Jacobi method, also useful for analyzing large fluctuations in population dynamics [52–55], we constructed a formal solution for the multivariate size

distribution. Moreover, the cumbersome rate equations reduce to a single second order differential equation, and numeric integration of this equations gives the percolation thresholds with, essentially, arbitrary accuracy.

Our analysis shows that the rate equation description extends to a broader class of evolving random graphs. Certainly, the multivariate aggregation analysis can be generalized to situations where the linking rate is degree

dependent. The multivariate aggregation framework can also be used to study the structure of clusters [56], and in particular, cycles.

We thank Wolfgang Losert for useful discussions. This research was supported by DOE grant DE-AC52-06NA25396 and NSF grant CCF-0829541.

-
- [1] R. Solomonoff and A. Rapaport, *Bull. Math. Biophys.* **13**, 107 (1959).
- [2] P. Erdős and A. Rényi, *Publ. Math. Inst. Hungar. Acad. Sci.* **5**, 17 (1960).
- [3] B. Bollobás, *Random Graphs* (Academic Press, London, 1985).
- [4] S. Janson, T. Luczak and A. Rucinski, *Random Graphs* (John Wiley & Sons, New York, 2000).
- [5] S. Janson, D. E. Knuth, T. Luczak, and B. Pittel, *Rand. Struct. Alg.* **3**, 233 (1993).
- [6] B. Pittel, J. Spencer, and N. Wormald, *J. Combin. Theor. Ser. B* **67**, 111 (1996).
- [7] D. Stauffer and A. Aharony, *Introduction to Percolation Theory* (Taylor & Francis, London, 1992).
- [8] G. Grimmett, *Percolation* (Springer, Berlin, 1999).
- [9] P. J. Flory, *J. Amer. Chem. Soc.* **63**, 3083 (1941).
- [10] W. H. Stockmayer, *J. Chem. Phys.* **11**, 45 (1943).
- [11] P. J. Flory, *Principles of Polymer Chemistry* (Cornell University Press, Ithaca, 1953).
- [12] P. Grassberger, *Math. Biosci.* **63**, 157 (1983).
- [13] M. E. J. Newman, *Phys. Rev. E* **66**, 016128 (2002).
- [14] T. Tome and R. M. Ziff, *Phys. Rev. E* **82**, 051921 (2010).
- [15] S. S. Wasserman, *J. Math. Soc.* **5**, 61 (1977).
- [16] M. E. J. Newman, D. J. Watts, and S. H. Strogatz, *Proc. Nat. Acad. Sci.* **99**, 2566 (2002).
- [17] M. Girvan and M. E. J. Newman, *Proc. Natl. Acad. Sci.* **99**, 7821 (2002).
- [18] B. Bollobás, C. Borgs, J. T. Chayes, J. H. Kim, and D. B. Wilson, *Rand. Struct. Alg.* **18**, 201 (2001).
- [19] M. Herrera, S. McCarthy, S. Slotterback, E. Cephas, W. Losert, and M. Girvan, *Phys. Rev. E* **83**, 061303 (2011).
- [20] C. Dwork, D. Peleg, N. Peppenger, and E. Upfal, *SIAM J. Comp.* **17**, 975 (1988).
- [21] Y. Wang and X. Y. Li, *Mob. Net. Appl.* **11**, 161 (2006).
- [22] E. Ben-Naim and P. L. Krapivsky, *Phys. Rev. E* **71**, 026129 (2005).
- [23] A. A. Lushnikov, *Physica D* **222**, 37 (2006).
- [24] P. L. Krapivsky, S. Redner, and E. Ben-Naim, *A Kinetic View of Statistical Physics* (Cambridge University Press, Cambridge, 2010).
- [25] K. T. Balinska and L. V. Quintas, *J. Math. Chem.* **8**, 39 (1991).
- [26] A. Ruciński and N. C. Wormald, *Comb. Prob. Comp.* **1**, 169 (1992).
- [27] N. C. Wormald, *J. Alg.* **5**, 247 (1984).
- [28] R. W. Robinson and N. C. Wormald, *Rand. Struct. Alg.* **5**, 363 (1994).
- [29] G. Chartrand, *Introductory Graph Theory* (Dover, New York, 1984).
- [30] E. Ben-Naim and P. L. Krapivsky, *Phys. Rev. E* **83**, 061102 (2011).
- [31] E. Ben-Naim and P. L. Krapivsky, unpublished (2011).
- [32] M. von Smoluchowski, *Z. Phys.* **17**, 557 (1916).
- [33] S. Chandrasekhar, *Rev. Mod. Phys.* **15**, 1 (1943).
- [34] N.C. Wormald, In *Lectures on Approximation and Randomized Algorithms*, M. Karoński and H.J. Prömel (eds), pp. 73–155. PWN, Warsaw, 1999.
- [35] F. Leyvraz, *Phys. Rep.* **383**, 95 (2003).
- [36] More complicated clusters do occur, but they are very rare, e.g. in classical random graphs their total number scales logarithmically with system size, see e.g. [4, 22].
- [37] P. L. Krapivsky and E. Ben-Naim, *Phys. Rev. E* **53**, 291 (1996).
- [38] T. Matsoukas and C. L. Marshall, *EPL* **92**, 46007 (2010).
- [39] R. M. Ziff, M. H. Ernst, and E. M. Hendriks, *J. Phys. A* **16**, 2293 (1983).
- [40] E. Ben-Naim and P. L. Krapivsky, *J. Phys. A* **38**, L417 (2005).
- [41] V. I. Arnold, *Geometrical Methods in the Theory of Ordinary Differential Equations* (New York, Springer-Verlag, 1988).
- [42] J. D. Logan, *An introduction to Nonlinear Partial Differential Equations* (Hoboken, N.J., Wiley-Interscience, 2008).
- [43] I. M. Gelfand and S. V. Fomin, *Calculus of Variations* (Englewood Cliffs, N.J.: Prentice-Hall, 1963).
- [44] For a fixed set of final coordinates x_j , the initial coordinates y_j satisfy the backward evolution equations $dy_j/d\tau = \sum_{i=0}^{d-j-1} [(du/d\tau) x_{i+j+1} - x_{i+j}] p_i$.
- [45] F. Bashforth and J. C. Adams, *Theories of Capillary Action* (Cambridge University Press, London, 1883).
- [46] D. Zwillinger, *Handbook of Differential Equations* (Academic Press, London, 1989).
- [47] W. H. Press, S. A. Teukolsky, W. T. Vetterling, and B. P. Flannery, *Numerical Recipes*, (Cambridge University Press, Cambridge, 1992).
- [48] The density $c(t)$ is twice differentiable at the percolation point; the third derivative undergoes a jump [24].
- [49] H. E. Stanley, *Introduction to Phase Transitions and Critical Phenomena* (Oxford University Press, New York, 1971).
- [50] S. Redner, *A Guide to First-Passage Processes* (Cambridge University Press, New York, 2001).
- [51] M. Mobilia, P. L. Krapivsky, and S. Redner, *J. Phys. A* **36**, 4533 (2003).
- [52] M. I. Freidlin and A. D. Wentzell, *Random Perturbations of Dynamical Systems*, (Springer-Verlag, New York, 1998).
- [53] M. I. Dykman, E. Mori, J. Ross, and P. M. Hunt, *J. Chem. Phys.* **100**, 5735 (1994).
- [54] V. Elgart and A. Kamenev, *Phys. Rev. E* **70**, 041106

(2004).

- [55] A. Kamenev and B. Meerson, Phys. Rev. E **77**, 061107 (2008).
 [56] E. Ben-Naim and P. L. Krapivsky, J. Phys. A **37**, L189 (2004).
 [57] R. M. Ziff, E. M. Hendriks, and M. H. Ernst, Phys. Rev. Lett. **49**, 593 (1982).

Appendix A: Classical Random Graphs

This appendix briefly describes how to obtain relevant properties of the classical random graph, $d = \infty$, using the Hamilton-Jacobi formalism. The density of connected components with size k obeys [24]

$$\frac{dc_k}{dt} = \frac{1}{2} \sum_{l+m=k} lm c_l c_m - kc_k, \quad (\text{A1})$$

with the initial condition $c_k(0) = \delta_{k,0}$. The generating function $\mathcal{C}(x, t) = \sum_k c_k(t)x^k$ satisfies

$$\frac{\partial \mathcal{C}}{\partial t} + x \frac{\partial \mathcal{C}}{\partial x} = \frac{1}{2} \left(x \frac{\partial \mathcal{C}}{\partial x} \right)^2, \quad (\text{A2})$$

with the initial condition $\mathcal{C}(x, 0) = x$.

Using the momentum $p = \frac{\partial \mathcal{C}}{\partial x}$, the Hamiltonian is

$$H = xp - \frac{1}{2}(xp)^2. \quad (\text{A3})$$

The Hamiltonian does not depend explicitly on time. Hence, H is a conserved quantity and consequently, xp is also constant. The evolution equations are

$$\frac{dx}{dt} = x(1 - xp), \quad \frac{dp}{dt} = -p(1 - xp), \quad (\text{A4})$$

with the initial conditions $x(0) = y$ and $p(0) = 1$. We can verify that $d(xp)/dt = 0$, and therefore, $xp = y$. By integrating (A4), we obtain the coordinate and the momentum,

$$x = y e^{(1-y)t}, \quad p = e^{-(1-y)t}. \quad (\text{A5})$$

The evolution equation for generating function is

$$\frac{d\mathcal{C}(x, t)}{dt} = -H + p \frac{\partial H}{\partial p} = -\frac{1}{2}(xp)^2.$$

Hence, the generating function is a quadratic function of the initial coordinate,

$$\mathcal{C}(x, t) = y - \frac{1}{2}y^2 t, \quad (\text{A6})$$

with $x = y e^{(1-y)t}$.

The mass of the giant component, $g = 1 - \sum_k k c_k$, follows from the momentum p at $x = 1$. The conservation law $xp = y$ implies that $p = y$ if $x = 1$. In analogy with (32), we have $g = 1 - y$, and using (A4), we find a closed equation,

$$g = 1 - e^{-gt}. \quad (\text{A7})$$

There is a trivial solution $g = 0$, valid at all time, and a second nontrivial solution, $g > 0$, valid only when $t > 1$. The latter is physical when $t > 1$, and hence, the giant component emerges at time $t_g = 1$.

To obtain the critical size distribution, that is, the size density at $t = t_g$, we note that the critical generating function is given by $\mathcal{C}_g(x) = y - \frac{1}{2}y^2$ with $x = y e^{1-y}$. We then focus on the behavior for $x \rightarrow 1$. We substitute the expansion $1 - y = a_1(1 - x)^{1/2} + a_2(1 - y) + \dots$ into the equation $x = y e^{1-y}$, and solve for the coefficients a_1 and a_2 . This calculation gives

$$1 - y = [2(1 - x)]^{1/2} - \frac{2}{3}(1 - x) + \dots$$

This expansion, together with Eq. (A6), gives the leading behavior of the critical generating function,

$$\mathcal{C}_g(x) = \frac{1}{2} - (1 - x) + \frac{2\sqrt{2}}{3}(1 - x)^{3/2} + \dots, \quad (\text{A8})$$

in the limit $x \rightarrow 1$. Thus, the critical size distribution has the power-law tail [57]

$$c_k \simeq \frac{1}{\sqrt{2\pi}} k^{-5/2}, \quad (\text{A9})$$

as follows from the leading singular component $(1 - x)^{3/2}$.